ISSN 2706-655X Vol.6, Issue 3: 74-83, DOI: 10.25236/IJFET.2024.060310

A Study of Relation between Rotor Propeller Position and Radar Cross Section Based on FEKO

Xinjian Wang[1], Wenxin Ye[2]

[1]*School of Physics and Electrical Engineering, Harbin Normal University, Harbin, 150025, China*
[2]*School of Information and Electronic Technology, Jiamusi University, Jiamusi, 154007, China*

Abstract: *The purpose of this study is to analyze the variation of radar scattering cross-section (RCS) of UAVs, specifically focusing on the impact of propeller positions, polarizations, and frequencies. Models of UAVs with different propeller positions were constructed, and simulations were conducted using FEKO. Through the analysis of RCS, the following conclusions were drawn: Frequency has a significant impact on RCS, especially at 500MHz, and the trend of RCS increase and decrease of UAVs with different propeller positions remains stable. Changes in propeller positions and polarization directions lead to differences in RCS, and the relationship is nonlinear. The changes in RCS at 2GHz and 5GHz frequencies are more complex, but consistent trends can still be observed at specific locations and frequencies. The variations in maximum RCS and observation view are inconsistent, indicating that radar scattering behavior is affected by multiple factors. These results have important implications for the design and optimization of unmanned aerial systems and contribute to our understanding of electromagnetic wave interactions.*

Keywords: *Rotor, Radar Cross Section (RCS), propeller position detection*

1. Introduction

The drone industry is experiencing rapid growth, with drones becoming increasingly accessible and affordable [1], [2]. These unmanned aerial vehicles (UAV) are being utilized in various civil applications such as pizza delivery [1], [2] and package delivery [3]. Depending on their payload capability, drones can be used for tasks such as inspection, delivery, monitoring, and photography. However, it is important to note that drones can also be misused as potential weapons, as seen in instances of terrorist strikes [4]. Therefore, strict controls on unauthorized drone usage are crucial to maintain security and public safety.

Detecting and identifying drones is essential in preventing security breaches. Detection involves monitoring targets that may be suspicious and pose a threat to the security of a given environment. Identification refers to determining the category of the target, specifically identifying whether the target is a drone. Acoustic and thermal sensors have been employed for drone identification [5][6], but they can be costly, energy-intensive, and challenging to integrate into drones due to size and weight limitations. Radar, on the other hand, is considered a valuable sensor for detecting and classifying various targets in urban environments [7]. Using radar for drone detection offers advantages such as being unaffected by weather and lighting conditions, making it suitable for operational requirements [8].

Studies have indicated that small drones are designed with very low radar scattering cross-sections (RCS) [9][10]. In our project, we focus on examining the RCS of UAVs at different propeller positions. By studying the RCS at these specific locations, we aim to gain a more accurate understanding of the radar signals received by drones, while considering cost and technical limitations. This research will provide valuable insights and support for the detection and identification of drones.

2. The design of FEKO simulation parameters and the establishment of models.

The FEKO simulation setup involves conducting four separate simulations at different frequencies: 500 MHz, 1 GHz, 2 GHz, and 5 GHz. These frequencies were chosen to explore the behavior of the system across commonly used wireless communication bands.

The simulations utilize linear polarization, where the electric field vector oscillates in a specific direction. The starting angles for theta and phi are both set to 0, corresponding to the system's reference axis. The end angle for theta is set to 180, covering the hemisphere above and below the reference axis.

ISSN 2706-655X Vol.6, Issue 3: 74-83, DOI: 10.25236/IJFET.2024.060310

Similarly, the end angle for phi is set to 360, ensuring complete azimuthal coverage. Both theta and phi angles increment by 1 degree for each iteration, allowing for a fine-grained sampling of the radiation pattern.

The objective of the simulation is to analyze the far-field radiation pattern by calculating the fields in the plane wave incident direction. The far-field refers to the region where electromagnetic waves propagate as plane waves and can be observed at a significant distance from the source. Studying the far-field radiation pattern provides valuable insights into the system's directional characteristics, beamwidth, and gain at different frequencies.

The simulation includes five different models, each representing a specific propeller configuration:

1) Four propellers parallel to the axis: In this model, four propellers are positioned parallel to the system's reference axis. This configuration is commonly encountered in applications where propellers are aligned to generate thrust in a specific direction.

2) Four propellers perpendicular to the axis: This model consists of four propellers positioned perpendicular to the system's reference axis. Such a configuration might be used in applications where propellers need to generate lift or induce airflow in a cross-axis direction.

3) Three propellers parallel to the axis and one propeller perpendicular to the axis: This model combines three propellers aligned parallel to the reference axis with one propeller positioned perpendicular to it. This configuration could be employed in scenarios where a combination of axial thrust and lateral control is required.

4) Two propellers parallel to the axis and two propellers perpendicular to the axis: In this model, two propellers are positioned parallel to the reference axis, while two propellers are positioned perpendicular to it. This configuration could be relevant in applications where a balance between axial thrust and lateral stability is desired.

5) One propeller parallel to the axis and three propellers perpendicular to the axis: This model features one propeller positioned parallel to the reference axis and three propellers positioned perpendicular to it. Such a configuration might be used to achieve a balance between axial thrust and controlled maneuverability.

These propeller positions are denoted as a, b, c, d, and e, representing specific configurations: (1)one propeller is parallel to the axis and three propellers are perpendicular to the axis (Figure 1). (2) two propellers are parallel to the axis and two propellers are perpendicular to the axis (Figure 2). (3) three propellers are parallel to the axis and one propeller is perpendicular to the axis (Figure 3). (4) four propellers are perpendicular to the axis (Figure 4). (5) four propellers are parallel to the axis (Figure 5).

The maximum size is observed when four propellers are parallel to the axis, while the minimum size is observed when four propellers are perpendicular to the axis. The maximum size measures x: 396.692 mm, y: 396.692 mm, and z: 68.78 mm. The minimum size measures x: 396.692 mm, y: 396.692 mm, and z: 68.78 mm.

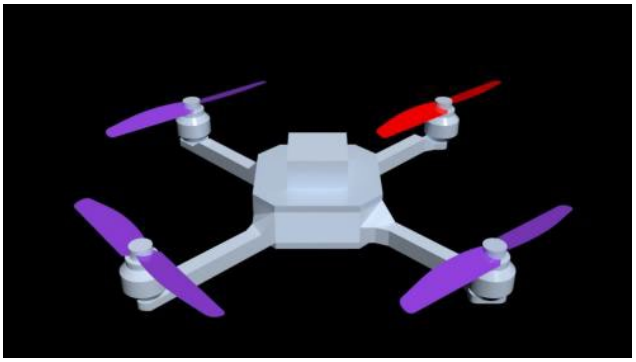

Figure 1: One propeller parallel to the axis and three propellers are perpendicular to the axis.

ISSN 2706-655X Vol.6, Issue 3: 74-83, DOI: 10.25236/IJFET.2024.060310

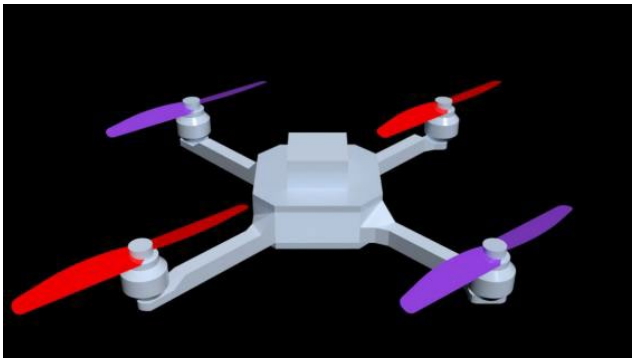

Figure 2: Two propellers parallel to the axis and two propellers perpendicular to the axis.

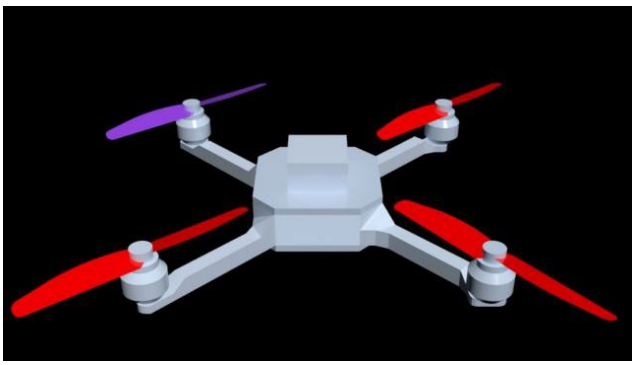

Figure 3: Three propellers parallel to the axis and one propeller perpendicular to the axis.

Figure 4: Four propellers perpendicular to the axis.

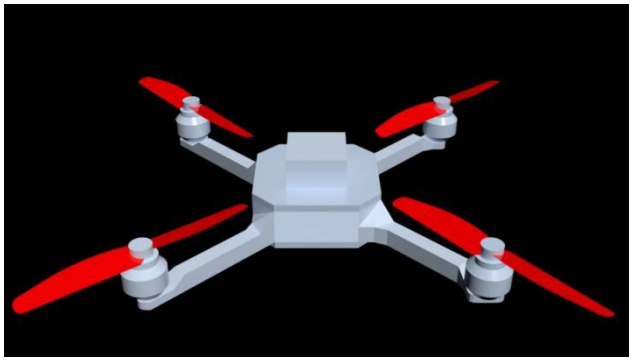

Figure 5: Four propellers parallel to the axis.

3. FEKO simulation results analysis

3.1 RCS of HH, HV/VH, VV for different propeller positions

RCS, or Radar Cross Section, is a measure of how much electromagnetic waves are scattered when

ISSN 2706-655X Vol.6, Issue 3: 74-83, DOI: 10.25236/IJFET.2024.060310

they encounter an object or structure [11]-[14]. In the context of this simulation, the propeller configurations act as scattering objects, and their RCS provides insights into how the system interacts with incident electromagnetic waves. The RCS of a target depends on various factors, including the viewing direction, frequency, and polarization of the radar signals, as well as the size, geometry, and composition of the target [15].

By analyzing the RCS of HH polarization, we can evaluate the system's response to horizontally polarized incident waves. This information helps us assess how the propeller positions reflect, absorb, or scatter the incident waves in different directions.

Similarly, the RCS of VV polarization focuses on the system's response to vertically polarized incident waves. By examining the RCS, we can understand how the different propeller positions affect the system's scattering characteristics for vertically polarized incident waves.

In the simulation, we analyze the RCS for HH (Horizontal-Horizontal), HV/VH (Horizontal-Vertical), and VV (Vertical-Vertical) polarizations for the various propeller positions.

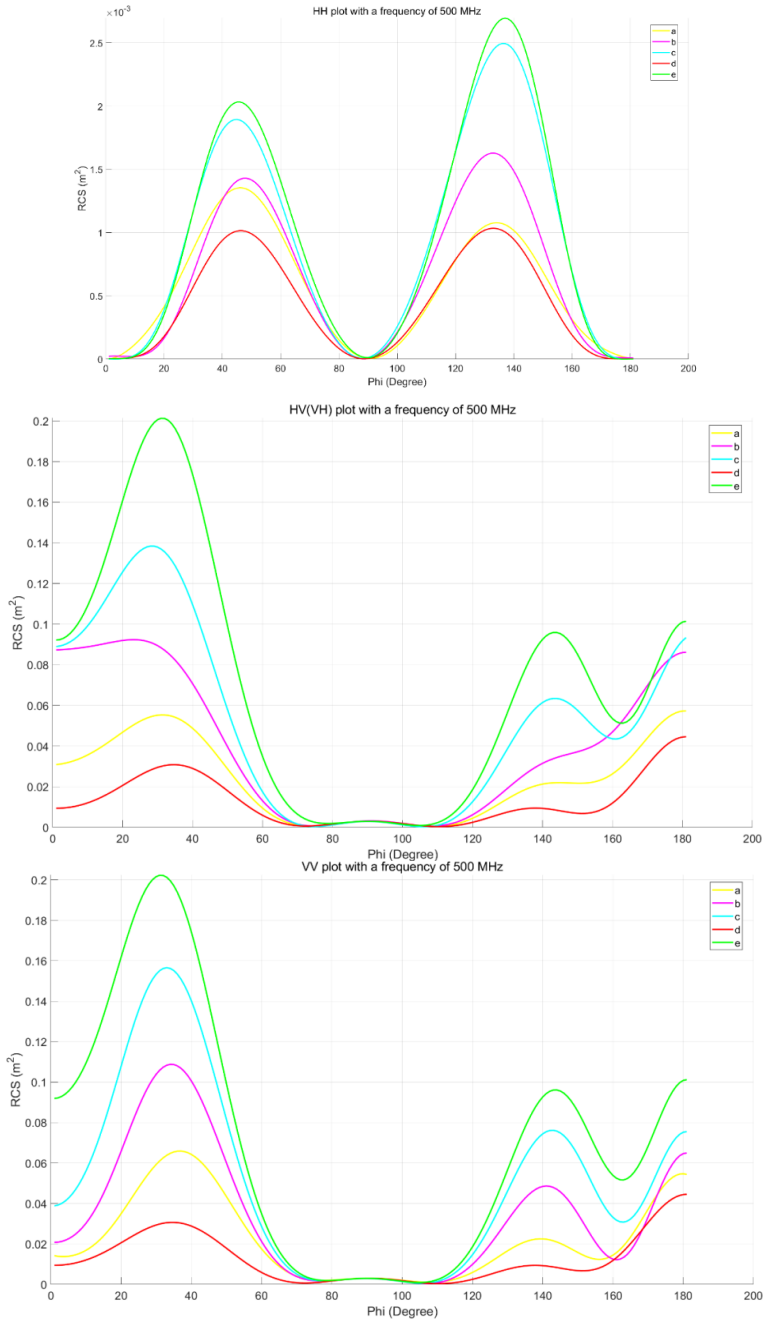

Figure 6: RCS diagram at 500MHz frequency

ISSN 2706-655X Vol.6, Issue 3: 74-83, DOI: 10.25236/IJFET.2024.060310

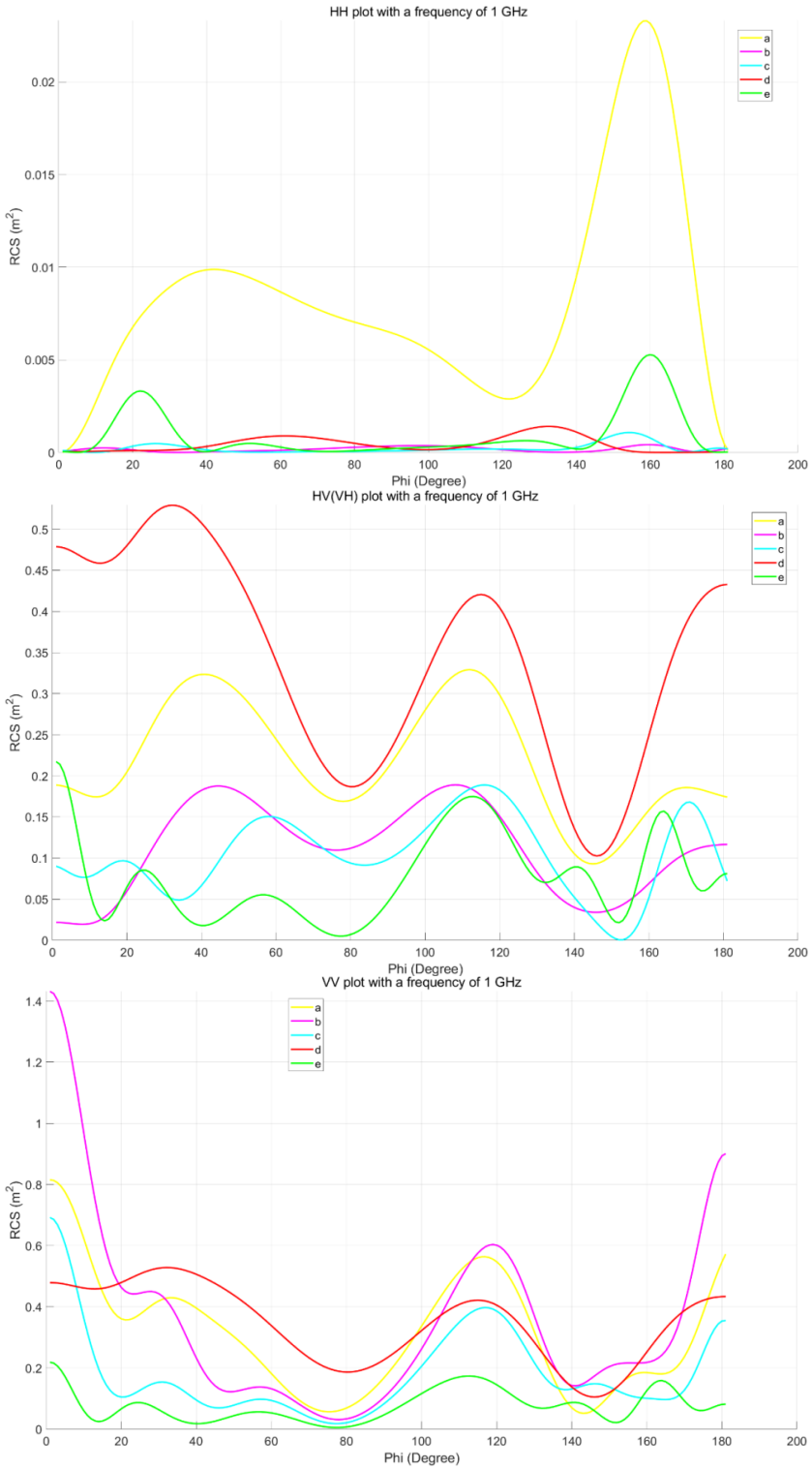

Figure 7: RCS diagram at 1GHz frequency

By analyzing Figure 6, we can observe the trend of RCS transformation at the 500 MHz frequency, which appears to be unaffected by changes in the propeller position. However, at certain specific frequencies, the impact of frequency on RCS may surpass that of the propeller position. This implies that regardless of how the propeller position changes, the properties of the radar wave at a frequency of 500 MHz will result in a similar trend in RCS.

At a frequency of 1 GHz and with HH polarization, the configuration of one propeller parallel to the axis and three propellers perpendicular to the axis exhibits the largest RCS. Figure 7 shows that the configuration of four propellers parallel to the axis also shows some fluctuations in RCS. However, the

ISSN 2706-655X Vol.6, Issue 3: 74-83, DOI: 10.25236/IJFET.2024.060310

remaining models barely receive any significant RCS.

Under HV/VH and VV polarizations, the reception of RCS by different models follows a similar trend of increasing and decreasing, similar to what was observed at approximately 500 MHz.

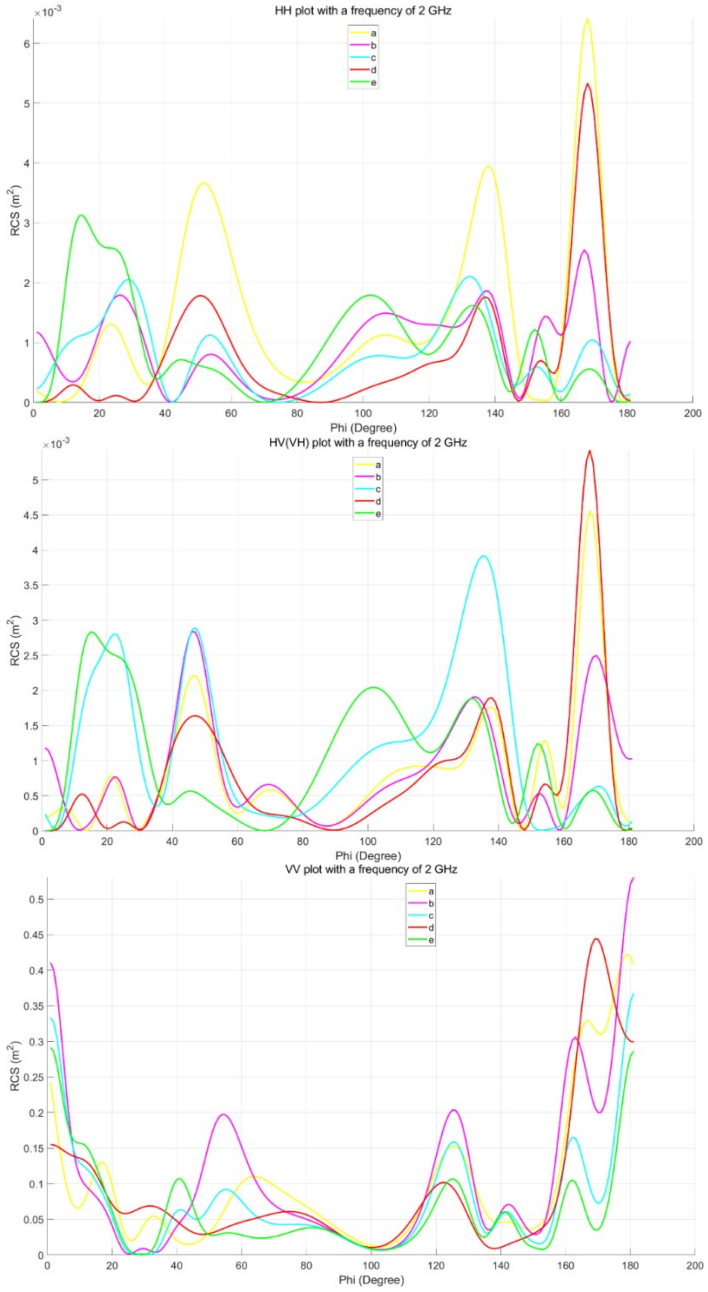

Figure 8: RCS diagram at 2GHz frequency

At the 2GHz frequency shown in Figure 8, the data for different polarizations shows a somewhat messy curve. However, there are specific locations where the curve exhibits a similar pattern of increasing and decreasing.

ISSN 2706-655X Vol.6, Issue 3: 74-83, DOI: 10.25236/IJFET.2024.060310

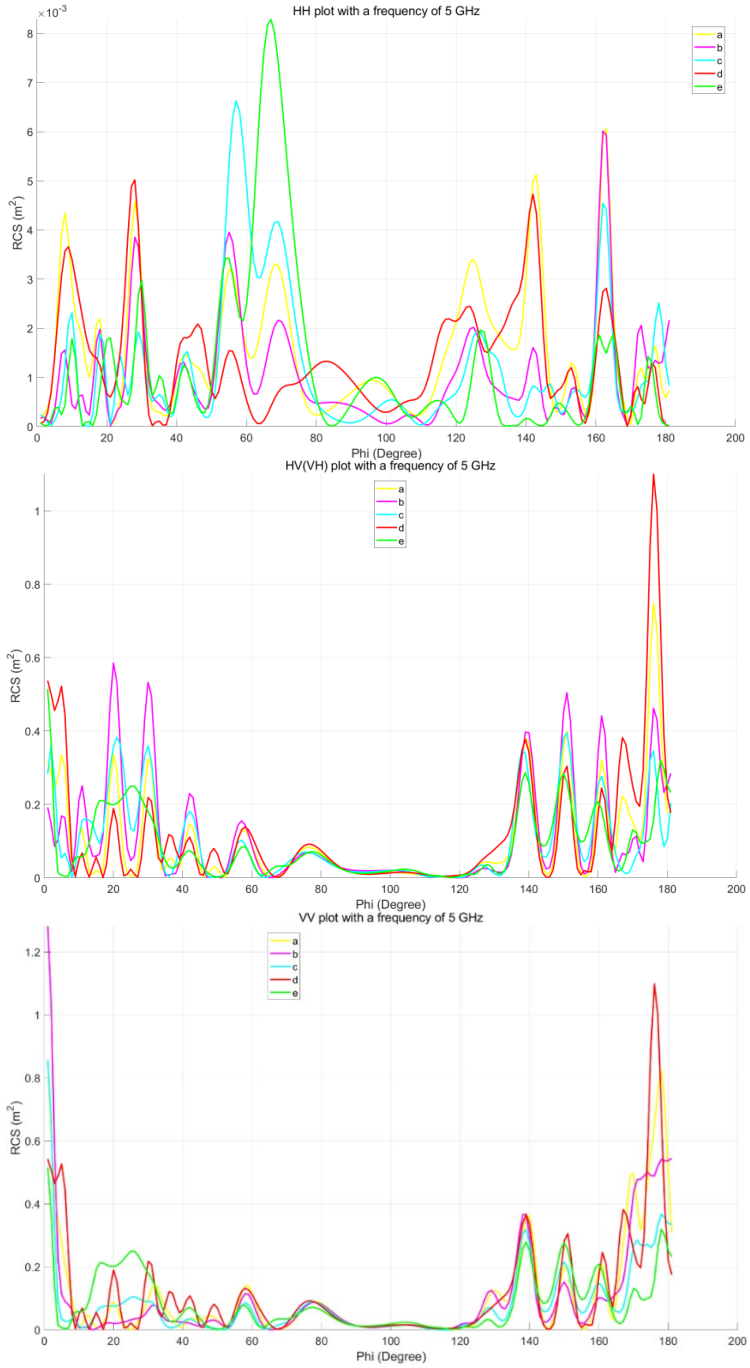

Figure 9: RCS diagram at 5GHz frequency

At the frequency of 5 GHz, figure 9 shows the amplitude of curve fluctuations is significantly larger. Under HV/VH and VV polarizations, the curve fit is high, indicating that changes in propeller position have a similar impact on the reception of RCS. However, under HH polarization, the amplitude of curve fluctuations is substantial, and there is no consistent pattern of increase or decrease as observed at the 500 MHz and 1/2 GHz frequencies.

Furthermore, it is observed that changing the position of two propellers does not result in a proportional change in RCS by a factor of two. Similarly, changing the position of four propellers does not lead to a proportional change in RCS by a factor of four. This suggests a non-linear relationship between propeller position and RCS.

The position where the maximum RCS occurs generally occurs when VV polarization occurs, that is, VV polarization has a greater impact on UAVs with different propeller positions.

RCS is influenced by various factors, including the UAV's geometry, material properties, and radar

ISSN 2706-655X Vol.6, Issue 3: 74-83, DOI: 10.25236/IJFET.2024.060310

frequency, which contribute to the complex and non-linear relationship observed. The calculation of RCS involves a combination of these factors, making it a complex phenomenon.

3.2 Observation View of Maximum RCS of VV, VH, and HH at different frequencies

Table 1: The maximum value of RCS at different frequencies at position a

	500MHz	1GHz	2GHz	5GHz
HH	45°	158°	167°	142°
HV(VH)	48°	136°	168°	140°
VV	45	0	180	177

Table 2: The maximum value of RCS at different frequencies at position b

	500MHz	1GHz	2GHz	5GHz
HH	132°	159°	166°	161°
HV(VH)	134°	47°	0°	9°
VV	132°	0°	180°	0°

Table 3: The maximum value of RCS at different frequencies at position c

	500MHz	1GHz	2GHz	5GHz
HH	135°	153°	131°	56°
HV(VH)	44°	116°	5°	68°
VV	135°	0°	180°	0°

Table 4: The maximum value of RCS at different frequencies at position d

	500MHz	1GHz	2GHz	5GHz
HH	132°	131°	167°	27°
HV(VH)	131°	127°	168°	142°
VV	132°	31°	169°	175°

Table 5: The maximum value of RCS at different frequencies at position e

	500MHz	1GHz	2GHz	5GHz
HH	136°	159°	13°	66°
HV(VH)	137°	159°	0°	66°
VV	137°	110°	180°	0°

Perform a detailed analysis of the data given in Tables 1-5:

1) Influence of Frequency on RCS:

Under HH polarization at position a, the RCS shows a slight increase between 500 MHz and 1 GHz. It then remains relatively stable at 2 GHz and increases again at 5 GHz. This behavior can be attributed to the stronger scattering effect of objects on electromagnetic waves at lower frequencies. At higher frequencies, other factors such as detailed features or wavelength limitations may restrict the scattering effect.

For HV (VH) polarization at position b, the RCS exhibits a significant decline between 1 and 2 GHz, followed by a subsequent increase at 5 GHz. This variation can be explained by the interaction between the object's geometry and the electromagnetic waves within that specific frequency range, leading to changes in the scattering response.

2) Comparison of RCS at Different Locations:

At 500 MHz, position a demonstrates the highest RCS for HH polarization, while position d exhibits the lowest RCS for HH polarization. This discrepancy can be attributed to position A's stronger reflection or scattering of electromagnetic waves at that particular frequency, whereas the object at position d may possess certain characteristics (e.g., shape or material) that result in a lower scattering response.

At 2 GHz, position c displays the highest RCS for HH polarization, suggesting that objects at this

ISSN 2706-655X Vol.6, Issue 3: 74-83, DOI: 10.25236/IJFET.2024.060310

location have optimal geometry for interaction with electromagnetic waves at that frequency.

3) Polarization Comparison:

Under VV polarization, positions a and b yield higher RCS, indicating strong reflection or scattering effects on vertically polarized electromagnetic waves.

Under HV (VH) polarization, positions a and d result in relatively lower RCS, implying a weaker response to horizontally and vertically polarized electromagnetic waves.

4) Outlier Analysis:

For VV polarization at position b, RCS values of 0° are observed at 1 GHz and 5 GHz. This suggests minimal reflection or scattering effects of the object on vertically polarized electromagnetic waves at these frequencies.

In the case of HV (VH) polarization at position d, an RCS value of 0° is observed at 2 GHz, indicating a very weak reflection or scattering effect on horizontally and vertically polarized electromagnetic waves at that specific position and frequency.

4. Conclusions

Based on the analysis of RCS for different propeller positions and polarizations, the following conclusions can be drawn:

1) Frequency Influence: The RCS demonstrates distinct trends with changing frequencies. At 500 MHz, the RCS remains consistent regardless of propeller position, indicating that frequency dominates RCS. However, at higher frequencies (1 GHz, 2 GHz, and 5 GHz), the RCS fluctuates and exhibits different patterns for different polarizations and propeller positions. This suggests that at these frequencies, propeller position and geometry play a more significant role in the scattering characteristics.

2) Propeller Position and Polarization: The RCS varies depending on the propeller position and polarization. At 1 GHz, under HH polarization, the configuration with one propeller parallel to the axis and three perpendicular propellers receives the largest RCS. Similarly, under HV/VH and VV polarizations, the RCS shows a similar increasing and decreasing trend around 500 MHz for different propeller positions. These findings highlight the influence of propeller position and polarization on the system's scattering characteristics.

3) At 5 GHz, the RCS curves show significant amplitude fluctuations. Under HV/VH and VV polarizations, the curves fit well, indicating consistent RCS reception with changing propeller positions. However, under HH polarization, the amplitude of fluctuation is large, and there is no consistent pattern observed at 500 MHz, 1 GHz, and 2 GHz frequencies.

4) Polarization Influence: The maximum RCS varies with different polarizations at each frequency and propeller position. For VV polarization, the maximum RCS is consistently high across all frequencies and positions, except for 1 GHz at position b, where it drops to 0°. This indicates a strong response to vertically polarized incident waves in most scenarios. However, for HH and HV (VH) polarizations, the maximum RCS shows more variability at different frequencies and positions, suggesting different scattering behaviors for horizontal and mixed polarizations.

Changes in propeller positions and polarization directions cause RCS variations, but no clear linear relationship exists. At 2 GHz and 5 GHz, RCS changes become more complex, yet some locations and frequencies show similar trends. Inconsistent changes in maximum RCS and Phi suggest that radar scattering behavior is influenced by multiple factors.

Overall, the impact of propeller position on RCS is more pronounced at lower frequencies, while it becomes less significant at higher frequencies. Once the frequency reaches a certain point, the RCS value becomes independent of the UAV propeller position.

References

[1] Dominos DomiCopter pizza Deivery, [online] Available: httrc/zwww.voutubc. cotn/watch?v=ZDXuGQRpvs 4:1-2.
[2] Dodo pizza copter exprss dleivery, [online] Available: http://rt.com/news/167936-russia-drones-pizza-deliveryl:1-3.

ISSN 2706-655X Vol.6, Issue 3: 74-83, DOI: 10.25236/IJFET.2024.060310

[3] Amazon Prime Air, [online] Available: http://www.amazon.com/h?node=8037720011:1-3.
[4] Tomasz Zwęgliński, "The use of drones in disaster aerial needs reconnaissance and damage assessment-three-dimensional modeling and orthophoto map study"[J]. Sustainability, vol. 12, no. 15, pp. 6080, Jul 2020:3-17.
[5] Mezei, József, Viktor Fiaska and András Molnár, "Drone sound detection"[C], 2015 16th IEEE International Symposium on Computational Intelligence and Informatics (CINTI), 2015:2-9.
[6] Petar Andraši et al., "Night-time detection of uavs using thermal infrared camera"[J].Transportation Research Procedia, Jan 2017:1-7.
[7] Wang F, Liu P, Wei Z. Simulation Study About the Radar Cross Section of a Typical Targets Based on FEKO[J]. Lecture Notes in Electrical Engineering, 2021. DOI:10.1007/978-981-15-8411-4_205.
[8] P. Poitevin, M. Pelletier and P. Lamontagne, "Challenges in detecting UAS with radar"[C].2017 International Carnahan Conference on Security Technology (ICCST), 2017:4-7.
[9] I. Guvenc, F. Koohifar, S. Singh, M. L. Sichitiu and D. Matolak, "Detection tracking and interdiction for amateur drones"[C].IEEE Commun. Mag., Apr. 2018:1-15.
[10] M. Ezuma, O. Ozdemir, C. Kumar, W. A. Gulzar and I. Guvenc, "Micro-UAV detection with a low-grazing angle millimeter wave radar"[C].Proc. IEEE Radio Wireless Week (RWW) Conf., Jan. 2019:9-15.
[11] U. F. Knott, "Radar Cross Section Measurements"[M]. New York: Van Nostrand Reinhold, 1993:6-17:1-23.
[12] J. F. Shaeffer, M. T. Tuiey and E. F. Knot, Radar Cross Section[M]. MA, Norwood: Artech House, 1985:3-15.
[13] C. Jenn, "4" in Radar and Laser Cross Section Engineering [M].VA, Reston: A1AA, 1995:7-19.
[14] Wang C , Wang Y , Wang W ,et al.Electromechanical coupling based influence of structural error on radiation and scattering performance of array antennas[J].Electronics Letters, 2017, 53(14):904-906.DOI:10.1049/el.2017.1072.
[15] C. Uluisik, G. Cakir, M. Cakir and L. Sevgi, "Radar cross section (RCS) modeling and simulation, part 1: a tutorial review of definitions, strategies, and canonical examples"[J]. In IEEE Antennas and Propagation Magazine, Feb. 2008:2-21.